Stem Cell Research (2011) 7, 124–136

available at www.sciencedirect.com

ScienceDirect

www.elsevier.com/locate/scr

REGULAR ARTICLE

Directed differentiation of porcine epiblast-derived neural progenitor cells into neurons and glia

M.A. Rasmussen [a,*], V.J. Hall [a], T.F. Carter [b], P. Hyttel [a]

[a] Department of Basic Animal and Veterinary Sciences, Faculty of Life Sciences, University of Copenhagen, Groennegaardsvej 7, DK-1870 Frederiksberg C, Denmark
[b] Department of Biomedical Sciences, University of Guelph, 50 Stone Road East, N1G 2W1, Guelph, Ontario, Canada

Received 2 August 2010; received in revised form 21 April 2011; accepted 29 April 2011
Available online 7 May 2011

Abstract Neural progenitor cells (NPCs) are promising candidates for cell-based therapy of neurodegenerative diseases; however, safety concerns must be addressed through transplantation studies in large animal models, such as the pig. The aim of this study was to derive NPCs from porcine blastocysts and evaluate their in-vitro differentiation potential. Epiblasts were manually isolated from expanded hatched blastocysts and cultured on MEF feeder cells. Outgrowth colonies were passaged to MS5 cells and rosettes were further passaged to Matrigel-coated dishes containing bFGF and EGF. Three NPC lines were established which showed expression of SOX2, NESTIN and VIMENTIN. One line was characterised in more detail, retaining a normal karyotype and proliferating for more than three months in culture. Following differentiation, *TUJI* was significantly up-regulated in protocol 2 (RA and SHH; 58% positive cells) as were *NF* and *TH*. In contrast, *MBP* was significantly up-regulated in protocol 3 (FGF8 and SHH; 63% positive cells), whereas, *GFAP* was significantly up-regulated in protocols 1–4 (33%, 25%, 43% and 22%). The present study provides the first report of a porcine blastocyst-derived NPC line capable of differentiating into both neurons and glia, which may be of paramount importance for future transplantation studies in large animal models of neurodegenerative diseases.

Introduction

Neural progenitor cells (NPCs) can be induced to form neurons, astrocytes and oligodendrocytes by either instructive paracrine cues, or by selective survival mechanisms (Mehler and Kessler, 1999). When isolated and cultured in-vitro, NPCs are capable of long-term culture in the presence of basic fibroblast growth factor (bFGF) and epidermal growth factor (EGF) (Andersen et al., 2009). In the human fetal brain, the majority of NPCs are located in the cerebral cortical ventricular zone (VZ) and in the subventricular zone (SVZ) of the lateral ventricular wall. In the adult brain, they are also present in the subgranular zone (SGZ) of the hippocampal dentate gyrus (Ma et al., 2009). Human NPCs are characterized by expression of the transcription factors *SOX2* and *PAX6*, the intermediate filament *NESTIN*, as well as the RNA binding protein *MUSASHI* (Ma et al., 2009; Maisel et al., 2007). However, the

Abbreviations: AA, Ascorbic acid; BDNF, Brain-derived neurotrophic factor; bFGF, Basic fibroblast growth factor; ESC, Embryonic stem cell; FGF8, Fibroblast growth factor 8; GDNF, Glial cell line-derived neurotrophic factor; ICM, Inner cell mass; iPSC, Induced pluripotent stem cell; LIF, Leukemia inhibitory factor; MEF, Mouse embryonic fibroblast; MPTP, 1 - methyl 4 - phenyl - 1, 2, 3, 6 - tetrahydropyridine; MS5, Mouse stromal cell line 5; MZ, Marginal zone; NPC, Neural progenitor cell; OC, Outgrowth colony; PDGF, Platelet-derived growth factor; RA, Retinoic Acid; SHH, Sonic Hedgehog; SGZ, Subgranular zone; SZ, Subventricular zone; VZ, Ventricular zone.

* Corresponding author. Fax: +45 353 32547.
E-mail address: miras@life.ku.dk (M.A. Rasmussen).

1873-5061/$ - see front matter © 2011 Elsevier B.V. All rights reserved.
doi:10.1016/j.scr.2011.04.004

transcriptional profile of fetal and adult NPCs does differ, indicating a fundamental difference in the way these cells may maintain their neuroprogenitor state (Maisel et al., 2007). Human NPCs can also be established from pluripotent cells in-vitro, such as embryonic stem cells (ESCs), which represent an attractive alternative to brain-derived NPCs due to the potential to generate unlimited amounts of cells. ESC-derived NPCs share many markers with their fetal counterparts such as expression of *SOX1*, *SOX2*, *NESTIN* and *MUSASHI* (Shin et al., 2007).

Research in rodents suggests that NPCs are interesting candidates for cell-based therapy of various neurodegenerative diseases. For example, transplantation of NPCs can improve cognition in a mouse model of Alzheimer's disease (Blurton-Jones et al., 2009), induce remyelination in a mouse model of multiple sclerosis (Pluchino et al., 2003) and improve locomotion and respiration in a rat model of Amyotrophic Lateral Sclerosis (Lepore et al., 2008). Several groups have furthermore shown that transplantation of ESC-derived dopaminergic neurons can restore motor function in a rat model of Parkinson's disease (Roy et al., 2006; Geeta et al., 2008; Yang et al., 2008). Although these studies represent a large step toward cell based-therapy in humans, there are considerable differences between rodent and human brain structure and function, including altered astrocyte activity (Oberheim et al., 2009) and brain aging processes (Oh et al., 2009). Furthermore, despite a general lack of tumor formation during allotransplantation in rodents, a documented case of a malignant tumor formation has been reported following transplantation of human NPCs into the brain of an Ataxia Telangiectasia patient (Amariglio et al., 2009). The large differences between rodent and human neurobiology underscore the need for more detailed non-rodent pre-clinical studies to understand and minimize the risks of NPC-transplantation.

Within the field of translational neuroscience, the pig is poised to become a pivotal biomedical model for testing the safety and potential of allotransplantation. The pig is an excellent candidate for this role, as it resembles man in size, anatomy and physiology (Lind et al., 2007); all of which are important aspects when studying diseases affecting a complex organ, such as the brain. The minipig is particularly ideal for studying Parkinson's disease, due to its similar anatomy within the substantia nigra (Nielsen et al., 2009) and development of Parkinsonian-like symptoms when treated with the neurotoxin MPTP (Bjarkam et al., 2008). In addition, the popularity of somatic cell nuclear transfer in livestock species facilitates the generation of transgenic pig models, such as the minipig model of Alzheimer's disease (Kragh et al., 2009). Establishment of transgenic NPC-lines from such in-vivo disease models would allow for detailed studies on disease mechanisms, as well as in-vitro drug screening.

The establishment of NPCs from pluripotent cells in ungulates, such as the pig, is currently hampered by the fact that ICM/epiblast cells cannot be maintained long-term in these species (Vackova et al., 2007). Hence, only a few studies have investigated the potential of in-vitro generated NPCs in large mammals. One study performed in a bovine system showed that neural crest progenitor cells could be derived directly from the inner cell mass (ICM) of in-vitro produced blastocysts (Lazzari et al., 2006). These cells could be maintained in-vitro for more than 112 days and when growth factors were withdrawn they differentiated into mature neural and glial subtypes, as well as chondrocytes and smooth muscle cells. In addition, Puy and co-workers have shown that rosettes generated from porcine ICM cells can give rise to NPCs, which could be maintained for up to 2 months in-vitro. However, the differentiation potential of these cells was limited to glial cells such as astrocytes and oligodendrocytes (Puy et al., 2010). Recent reports on the generation of porcine induced pluripotent stem cells (iPSCs) are opening new exciting possibilities for the derivation of NPCs in the future (Esteban et al., 2009; Ezashi et al., 2009; Wu et al., 2009).

To promote the development of the pig as a large animal model of NPC transplantation, a stable, porcine embryo-derived NPC line with the capacity to differentiate into both neural- and glial cells is required. The aim of the present study was: 1) to isolate and characterize NPCs from porcine epiblast cells and, 2) to evaluate whether the NPCs can be cultured long-term and differentiate into neural- and glial cells.

Results

Derivation of NPC lines from porcine epiblast cells

A timeline showing the derivation and differentiation of NPCs is presented in Fig. 1A. A total of 66 epiblasts were isolated from Day 9 expanded hatched blastocysts (Fig. 1B, C), classified according to Vejlsted and colleagues as early pre-streak I stage embryos containing a clear oval-shaped epiblast (Vejlsted et al., 2006) and cultured on mouse embryonic feeder (MEF) cells. On Day 4, 34 outgrowth colonies (OCs) had formed (52%). Some of the OCs grew as a central dense core, resembling the embryonic epiblast, surrounded by a monolayer of presumptive hypoblast cells, whereas, others grew in a monolayer of ESC-like cells (Fig. 1D, suppl. Fig. 1A, J). Both types of OCs presented typical ESC-like morphology with a large nuclear–cytoplasmic ratio containing one or two prominent nucleoli and showed nuclear-specific staining of OCT4. To promote neural differentiation, OCs were co-cultured with mouse MS5 stromal cells, which have previously been reported to improve neural differentiation of human ESC due to secretion of neurogenic factors (Barberi et al., 2003). Around Day 12–17, round or elongated rosettes with a central lumen started to form in the OCs (Fig. 1E, suppl. Fig. 1B, K). When rosettes were isolated and cultured in Matrigel-coated dishes in N2 medium containing bFGF and EGF, a population of cells rapidly grew out (Fig. 1F, suppl. Fig. 1C, L), which presented a bipolar morphology with large nuclei containing two or more prominent nucleoli (Fig. 1G). After the first passage, the cells attained a uniform morphology and neurospheres formed spontaneously during the first three passages or when cultured in non-coated dishes (Fig. 1H). When bFGF and EGF were withdrawn from the medium, the cells obtained a neuronal-like morphology with protrusions extending from individual soma (Fig. 1I).

Proliferation and karyotyping of NPCs

Three individual NPC lines were established, of which one was subjected to detailed characterization. Cell doublings

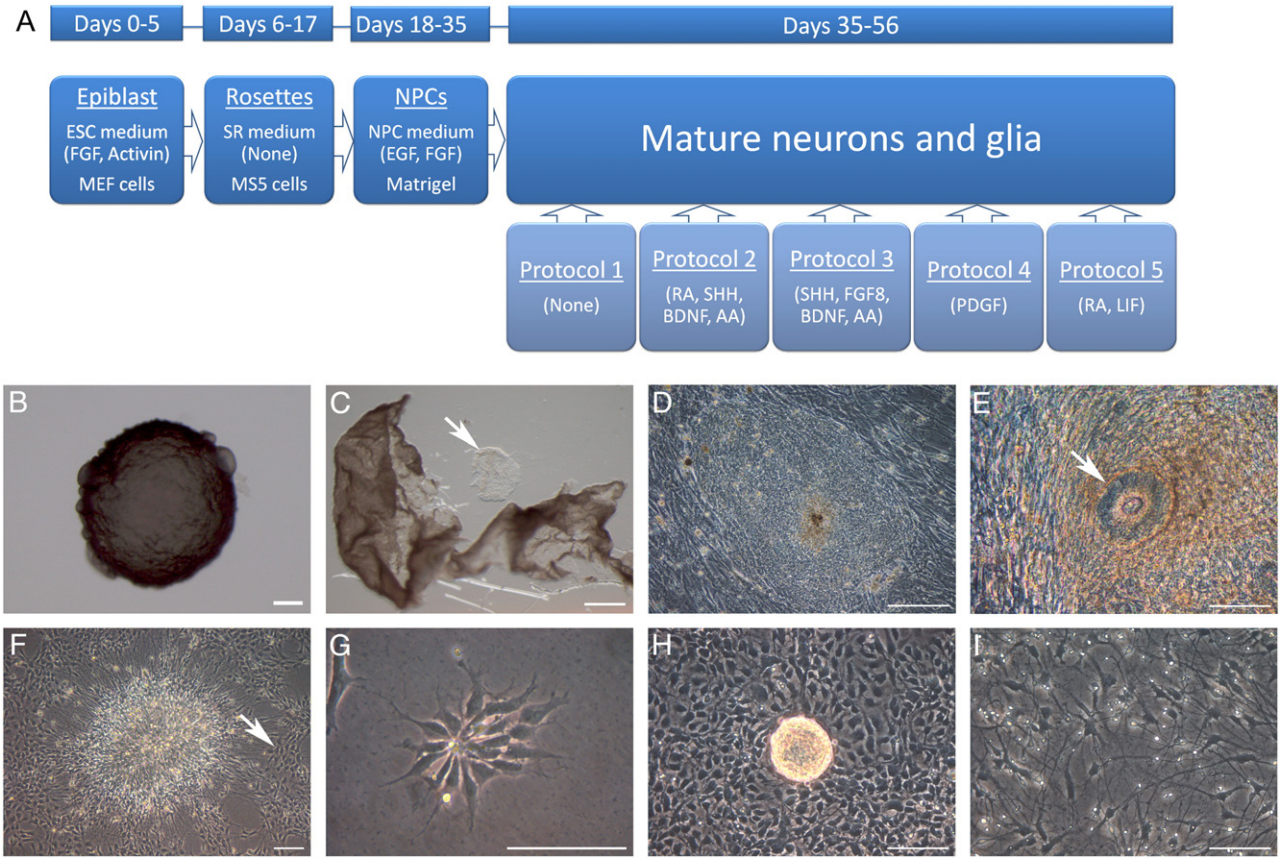

Figure 1 Derivation and morphology of neural progenitor cells. (A) Timeline showing the sequential steps for derivation of neural progenitor cells (NPCs) from porcine epiblast cells and the five different protocols used for generation of neural- and glial cells. (B) Expanded hatched blastocyst on Day 9. (C) Isolation of epiblast from the surrounding trophectoderm. Arrowhead points to an isolated epiblast. (D) Epiblast monolayer outgrowth colony grown for 5 days on mouse embryonic feeder (MEF) cells. (E) Neural rosette formed from epiblast cells after 17 days culture on MEF and MS5 feeder cells. Arrow points to a rosette structure. (F) Neural rosette isolated and cultured in Matrigel-coated dishes in NPC medium containing bFGF and EGF. Arrow points to outgrowing NPCs. (G) Closeup of NPCs derived from neural rosettes. (H) Neurosphere spontaneously formed during passage 3. (I) Neuronal-like morphology of NPCs cultured in medium without bFGF and EGF. Scale bars represent 0.1 mm.

were monitored over time by counting individual cells at passage from 1 to 15. Initially, the proliferation rate of the NPCs was exceptionally high with around 10 doublings each passage, however, at later passages this decreased to around 2.5 doublings for each passage, which remained relatively stable (Fig. 2A). The proliferation marker KI67, which was examined by immunocytochemistry, was expressed in 55.8% of the NPCs at passage 3 (Fig. 2B–D). Cytogenetic analysis of NPCs at passage 7 revealed a normal 38, XX karyotype with all analyzed metaphases free of any discernable cytogenetic abnormalities (Fig. 2E). The cells have been maintained for more than three months (30 passages) without losing their proliferative potential.

Comparative real-time PCR analysis of NPCs

To determine the nature of the NPCs, the cells were analyzed at passage 5, 21 and 30 by comparative real-time PCR. Reactions were performed with porcine specific primers of NPCs and mature neurons and glia, based on previous characterization of human NPCs. All reactions yielded a single transcript and amplicons were confirmed by sequencing. Reference genes tested on all the samples detected consistent levels of transcripts, indicating integrity of the cDNA samples (Suppl. Fig. 4). *GAPDH*, which was determined to be the most optimal reference gene, was subsequently used for normalization.

Expression of the transcription factor *SOX2* was three fold higher at passage 5 compared to fetal brain (control tissue) (Fig. 3A). At passage 21, this level was around 1.5 and at passage 30 it was around 1, indicating some down-regulation, despite maintaining a relatively high expression. The intermediate filament *NESTIN* was four and five folds higher than the control tissue at passage 5 and 21, respectively, but showed a decrease to around 2 fold at passage 30 (Fig. 3B). In contrast, the intermediate filament *VIMENTIN* was more stable, showing 8 to 13 folds higher expression of transcripts than the control tissue at all the examined stages (Fig. 3C). *BETA-TUBULIN III* (*TUJI*), considered a marker of immature neurons, was almost undetectable at all passages (Fig. 3D).

Immunocytochemical analysis of NPCs

Immunocytochemical analysis with an antibody against OCT4 (considered a marker of pluripotency in human and mice),

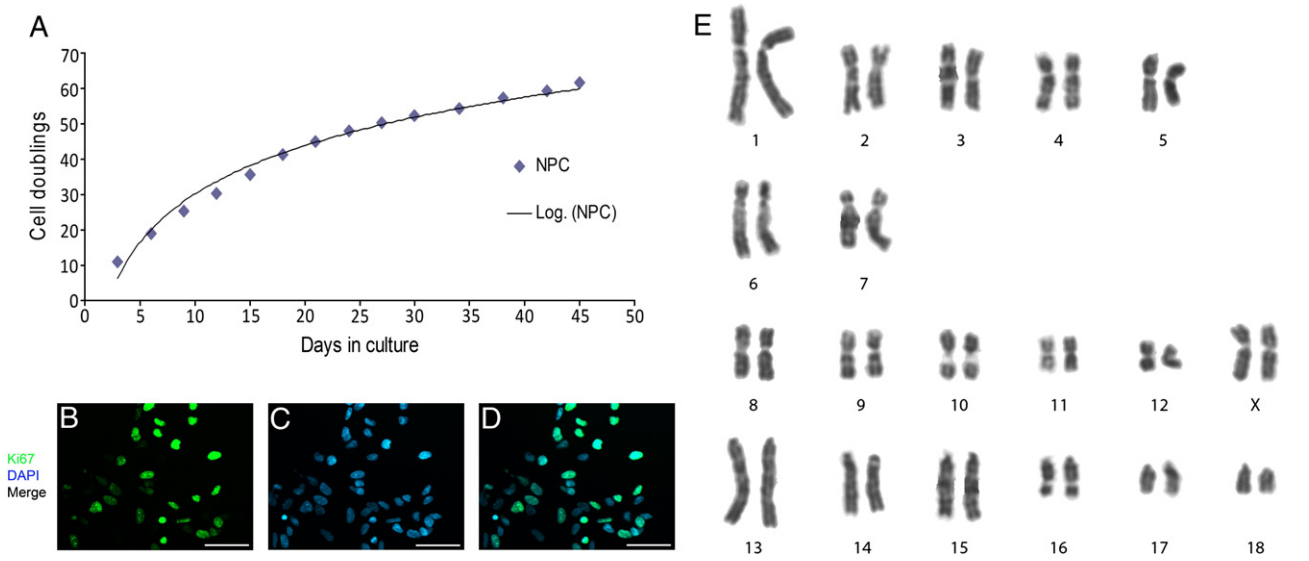

Figure 2 Proliferation and karyotyping of neural progenitor cells. (A) Total cell doublings of neural progenitor cells (NPCs), estimated by cell countings at each passage (3–4 days interval). (B) KI67 staining of NPCs at passage 3. (C) Hoechst staining of NPCs at passage 3. (D) Merge of B and C. Scale bars represent 0.05 mm. (E) A representative 38, XX karyotype prepared from passage 7 NPCs using standard cytogenetic techniques and Giemsa staining.

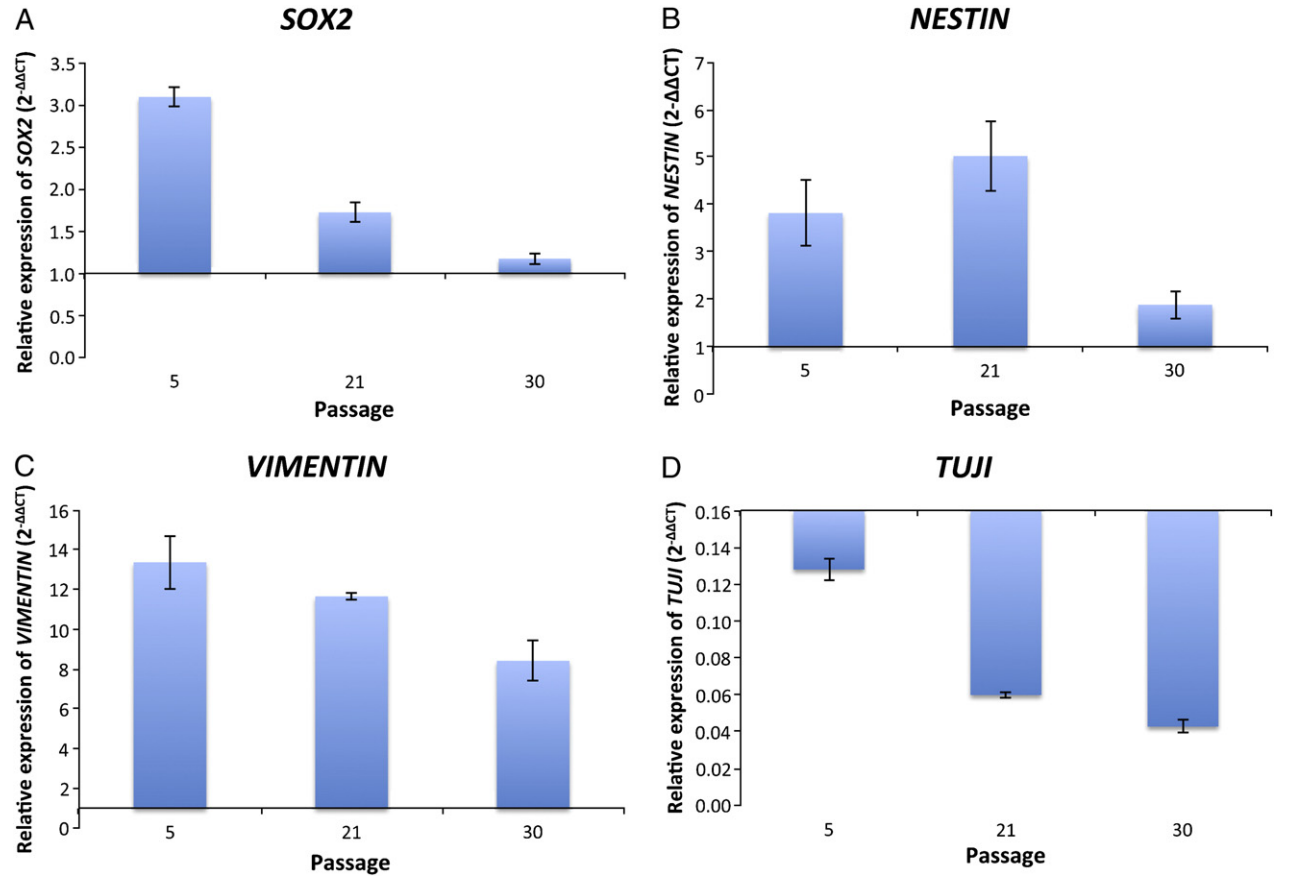

Figure 3 Comparative real-time PCR expression in neural progenitor cells (NPCs). Expression of NPC-markers in porcine NPCs at passage 5, 21 and 30. (A) *SOX2* expression. (B) *NESTIN* expression. (C) *VIMENTIN* expression. (D) *TUJI* expression. The expression was measured by comparative real-time PCR with Day 42 porcine brains as reference tissue. The experiments were performed in biological triplicates and normalized to the housekeeping gene *GAPDH*. Error bars represent the standard deviation of the mean.

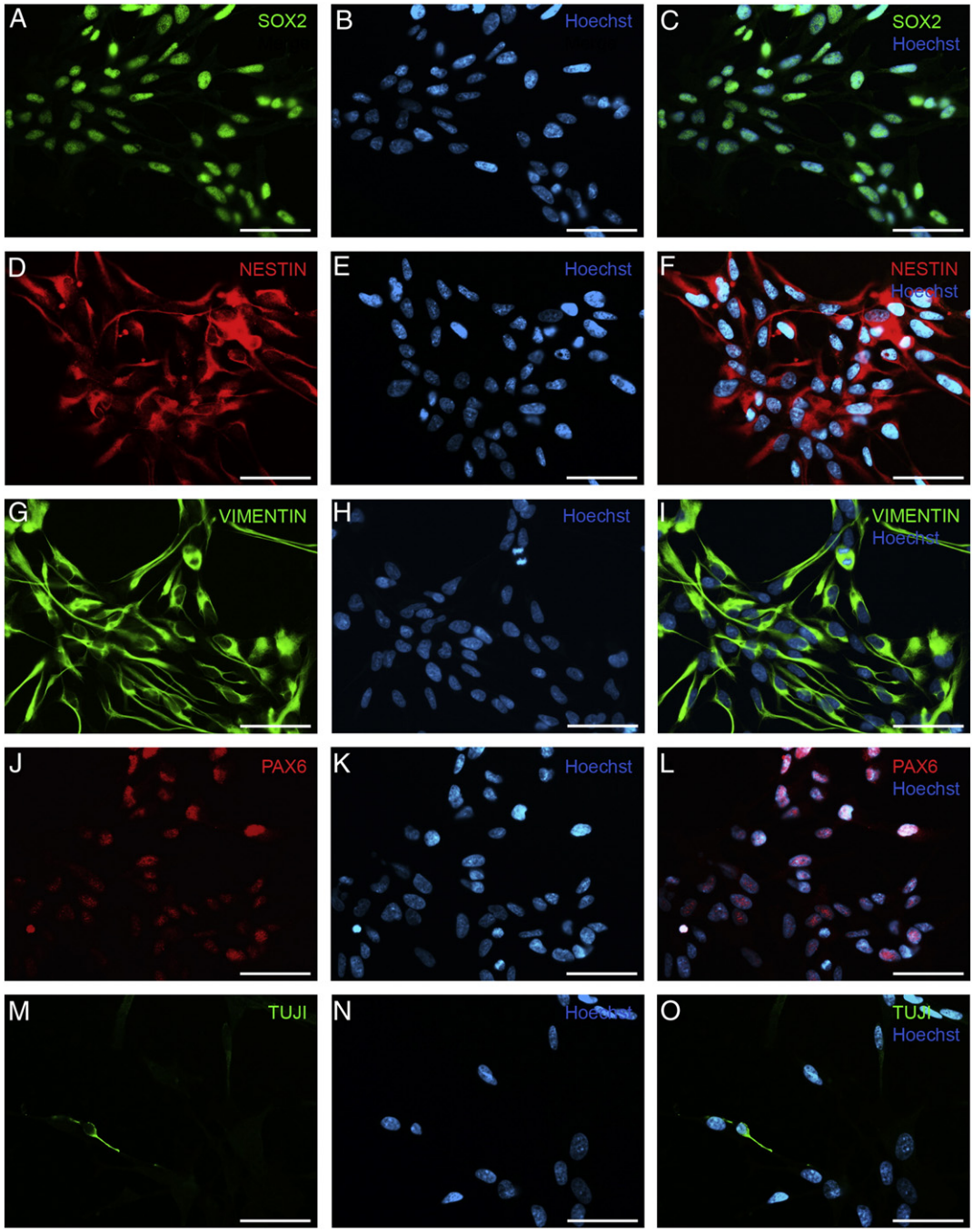

Figure 4 Immunocytochemistry of neural progenitor cells (NPCs). Staining of NPCs with NPC-markers at passage 3. (A) SOX2. (D) NESTIN. (G) VIMENTIN. (J) PAX6. (M) TUJI. (B, E, H, K, and N) Hoechst. (C, F, I, L and O) Merge of primary antibody staining and Hoechst. Scale bars represent 0.05 mm.

showed nuclear localized OCT4 labeling in OCs, whereas this marker was completely absent in the NPCs at passage 4 (data not shown). In contrast, quantitative immunocytochemical analyses showed nuclear localization of SOX2 in 99.3% of the NPCs at passage 4 (Fig. 4A–C). The NPCs also showed cytoplasmic localization of NESTIN (Fig. 4D–F) and VIMENTIN (Fig. 4G–I) in 96.0% and 99.6% of the examined cells, respectively. Furthermore, nuclear localization of PAX6 was observed in 99.1% of the cells (Fig. 4J–L). In contrast, TUJI (Fig. 4M–O) was localized to the cytoplasm in only 0.3% of the cells, and NCAM staining was negative (data not shown).

To further analyze the NPCs, staining's with GFAP and SSEA1 (considered markers of human radial glial cells) were carried out, however, in both cases these markers were negative (data not shown). The observed expression profile was confirmed for two additional NPC lines at comparable passages using immunocytochemistry (Suppl. Fig. 1D–I, M–R). Immunocytochemistry performed at passage 16 confirmed nuclear localization of SOX2 and cytoplasmic staining of NESTIN and VIMENTIN, whereas, PAX6 was low at this stage and a weak cytoplasmic TUJI staining was observed in a slightly higher percentage of the cells (Suppl. Fig. 2). Therefore, it would

seem that the cellular phenotype could be changing somewhat over extended culture periods.

Immunohistochemical analysis of Day 42 fetal brain

Immunohistochemical analysis of a Day 42 porcine fetal brain identified specific areas that showed localization of NPC-markers including the developing nasal conchae, the neural layer of the retina, and the ventricular zone (VZ) of the lateral ventricle (Fig. 5A). In the VZ, nuclear localization of KI67, SOX2, and PAX6 and cytoplasmic localization of NESTIN and VIMENTIN was observed (Fig. 5B–F), whereas, the surrounding marginal zone (MZ) displayed cytoplasmic localization of TUJI and NCAM (Fig. 5G–H), and GFAP was negative (data not shown). Localization of KI67, SOX2, PAX6, NESTIN, and TUJI was also observed in the developing nasal conchae and KI67, SOX2, PAX6, NESTIN, VIMENTIN, TUJI, and NCAM in the neural layer of the retina (data not shown).

Morphology of differentiated NPCs

To test the differentiation potential of the NPCs, five different protocols used for differentiation of human and mouse NPCs were applied. All the protocols comprised removal of bFGF and EGF from the culture media at passage 3 and addition of specific growth factors to promote the generation of different populations of neural- and glial cells. In protocol 1 (without growth factors for spontaneous differentiation of NPCs (Joannides et al., 2007)) the cells mainly attained a multipolar morphology with several protrutions extending from a single soma (Suppl. Fig. 3B). In protocol 2 (including RA, SHH, BDNF and AA for generation of motoneurons (Lee et al., 2007)) extensive clustering of cells with a bipolar morphology was apparent with large cytoplasmic protrutions extending from clusters of soma (Suppl. Fig. 3C). In protocol 3 (containing FGF8, SHH, BDNF and AA for generation of dopaminergic neurons (Perrier et al., 2004)) clustering of cells with a multipolar morphology was mainly observed and the culture was passaged on Day 9 due to continued proliferation (Suppl. Fig. 3D). In protocol 4 (containing PDGF for generation of oligodendrocytes (Hu et al., 2008)) cells with larger nuclei were mostly observed, often with wide, cytoplasmic protrusions (Suppl. Fig. 3E). Again, continued growth required the cells to be passaged on Day 9. Finally, in protocol 5 (containing RA and LIF for generation of astrocytes (Asano et al., 2009)) clustering of cells with a multipolar morphology was most predominant (Suppl. Fig. 3F).

Comparative real-time PCR analysis of differentiated NPCs

Comparative real-time PCR was performed at the end point of the differentiation experiment. *NESTIN* expression had decreased to around half the level of undifferentiated NPCs in Protocols 1 and 4, whereas, in the remaining protocols the levels were unaltered (Fig. 6A). The expression of the early neuronal marker *TUJI* was 10 and 5 fold higher than in undifferentiated NPCs in protocols 2 and 5, respectively, whereas this marker only showed a slight up-regulation in protocols 1, 3 and 4 (Fig. 6B). Only protocol 2 showed a significant difference from undifferentiated NPCs. The same expression profile was identified for markers of more mature neurons such as *NEUROFILAMENT* (*NF*) and *TYROSINE HYDROXYLASE* (*TH*), which were both significantly up-regulated in protocol 2 (Fig. 6C–D). *GFAP*, a marker of astrocytes, was around 100 fold higher in protocol 1, 2, 3 and 4, which was significantly different from undifferentiated NPCs (Fig. 6E). In contrast, *GFAP* was not statistically different from undifferentiated NPCs in protocol 5. Finally, a marker of oligodendrocytes, *MYELIN BASIC PROTEIN* (*MBP*), was tested; however, this marker was around the detection limit in fetal brain. Nevertheless, it was significantly up-regulated around 12 fold compared to undifferentiated NPCs in protocol 3, whereas, in the other protocols, *MBP* was only up-regulated between 1 and 5 fold (Fig. 6F).

Immunocytochemical analysis of differentiated cells

Immunocytochemical analysis and quantification of differentiated cells showed that cytoplasmic localization of NESTIN was still observed in 59%, 68%, 52%, 12% and 80% of

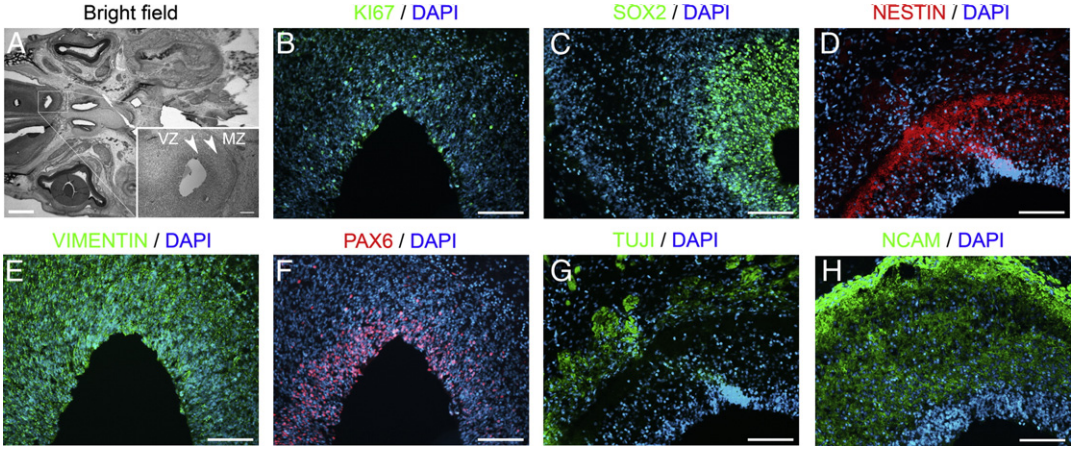

Figure 5 Immunohistochemistry of porcine fetal brain. Immunohistochemical staining of a porcine brain from a Day 42 fetus. (A) Morphology of the telencephalon, Scale bar represent 1 mm. Inset shows a close up of the lateral ventricle with arrows pointing to the ventricular zone (VZ) and the marginal zone (MZ), respectively. Scale bars represent 0.5 mm. (B–H) Antibody stainings of the VZ and MZ of the lateral ventricle. (B) KI67. (C) SOX2. (D) NESTIN. (E) VIMENTIN. (F) PAX6. (G) TUJI. (H) NCAM. Scale bars represent 0.1 mm.

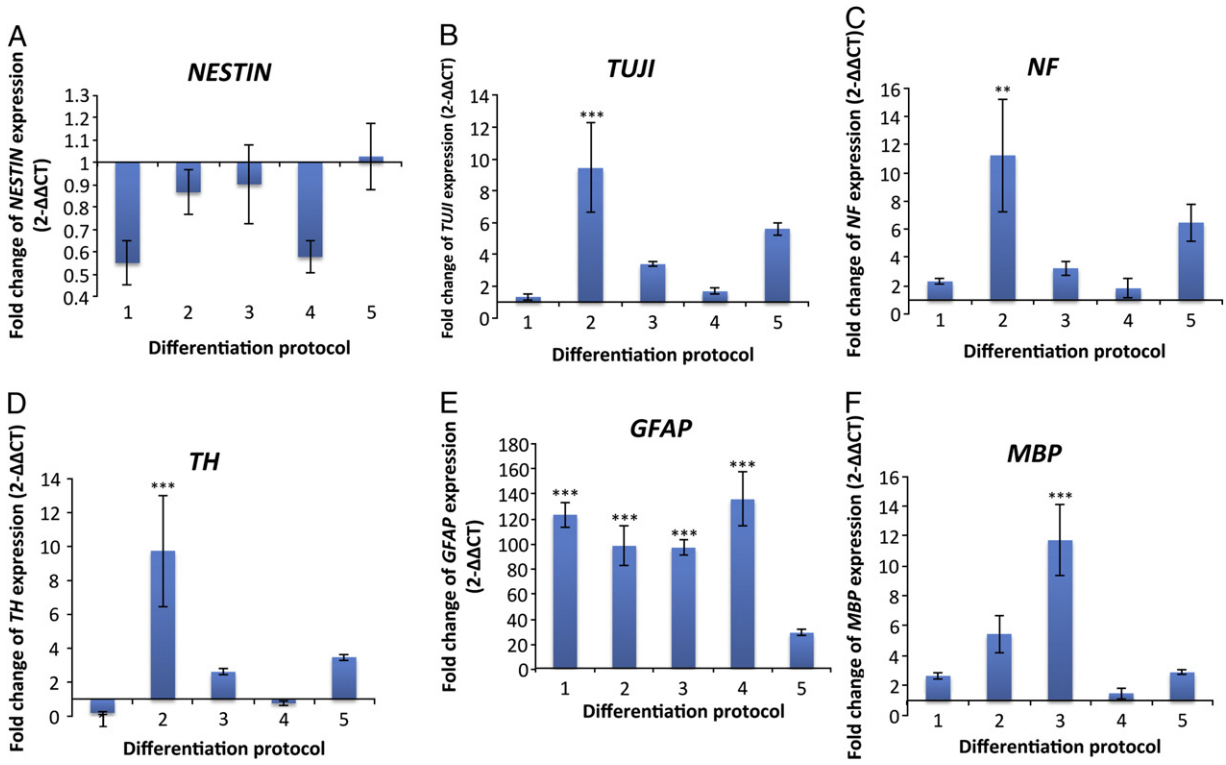

Figure 6 Comparative real-time PCR expression in differentiated cells. Expression of neural- and glial cell markers in neural progenitor cells (NPCs) submitted to five differentiation protocols (protocol 1–5). (A) *NESTIN*. (B) *TUJI*. (C) *NF*. (D) *TH*. (E) GFAP and (F) *MBP*. The expression was measured by comparative real-time PCR relative to the expression in undifferentiated NPCs. Samples were normalized to the housekeeping gene *GAPDH*. The experiments were performed in biological triplicates by differentiating the NPCs at passage 3. Significant difference from undifferentiated NPCs is indicated with different significance levels by ***=$p<0.001$, **=$p<0.01$ and *=$p<0.05$. Error bars represent the standard deviation of the mean.

the cells in protocols 1, 2, 3, 4 and 5, respectively, indicating that complete down-regulation of this marker did not occur (Fig. 7A–C). Cytoplasmic localization of TUJI was found in 34%, 58%, 29%, 21% and 80% of the cells in protocols 1–5, respectively (Fig. 7D–F), which corresponded relatively well with the observed expression profile of *TUJI*. In addition, cytoplasmic localization of TH was observed in protocol 2, but only in few cells (Fig. 7G–I). Cytoplasmic localization of GFAP was observed in 34%, 25%, 43%, 22% and 13% of the cells in protocols 1–5, respectively (Fig. 7J–L), which also corresponded more or less with the expression profile of this marker. Finally, cytoplasmic localization of O4, a marker of type I and II pro-oligodendrocytes but not of O-2A progenitor cells (Dhara et al., 2008), was observed in protocols 3 and 4 at 30% and 63% of the cells, respectively (Fig. 7M–O).

Discussion

The current study presents for the first time a porcine blastocyst-derived NPC line with the ability to differentiate into both neural- and glial cells. Co-culture of porcine epiblast cells with MS5 cells gave rise to formation of rosettes after 12–17 days in culture, which is comparable to ESCs cultured under the same conditions (Barberi et al., 2003; Perrier et al., 2004). The rosette-derived NPCs were cultured in the presence of bFGF, a well-known mitogen of neural specification, and EGF, which is reported to promote self-renewal of NPCs (O'Keeffe et al., 2009) and have currently been cultured for more than three months without losing their proliferative capacity.

An important feature of stem cells is their ability to grow indefinitely in culture; hence, to shed light on this issue, cell doublings were monitored over time. The NPCs were capable of more than 60 population doublings without ceasing to proliferate, although an initially high proliferation rate followed by a period of slower, yet stable proliferation was observed. This kind of growth is best described as logarithmic growth, which has previously been reported for human NPCs (Reubinoff et al., 2001). However, with the symmetrical divisions of undifferentiated NPCs, one would ideally expect an exponential growth, which has been reported in other studies (Lazzari et al., 2006; Hong et al., 2008).

KI67 staining at passage 3 showed that 55.8% of the NPCs expressed this proliferation marker, which is comparable to the 50% KI67 positive cells found by Puy et al. (2010). In comparison, human NPCs have been shown to express KI67 in 53.5% of the cells, whereas, mouse NPCs express KI67 in 80% of the cells (Sun et al., 2009), indicating that the NPCs have similar proliferation rate as human NPCs. The observation that the NPCs were karyotypically normal at passage 7 indicated that the culture conditions did not give rise to cytogenetic abnormalities at this stage of development.

The NPCs were positive for *SOX2*, *NESTIN* and *VIMENTIN* as detected by comparative real-time PCR and verified by

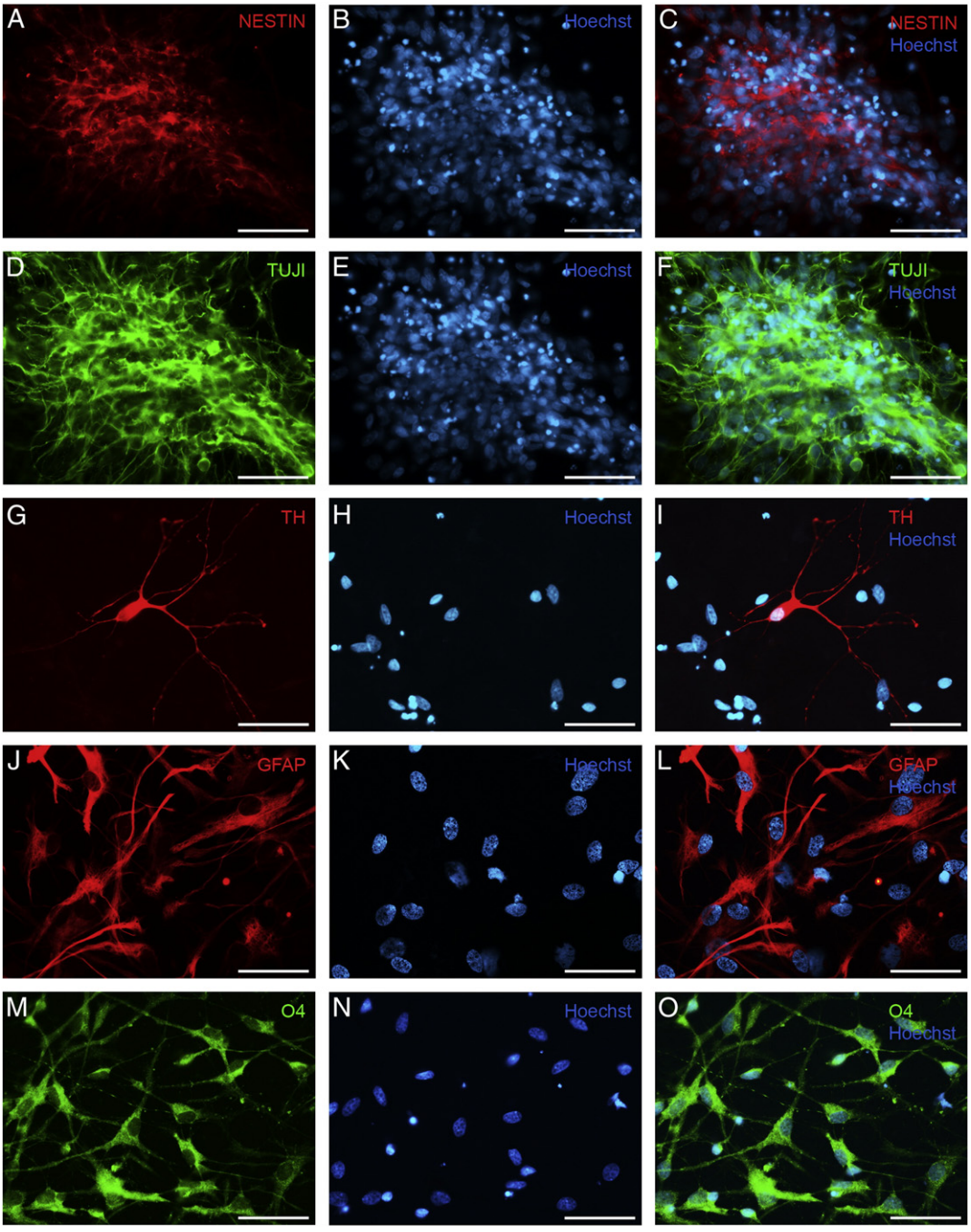

Figure 7 Immunocytochemistry of differentiated cells. Antibody stainings with neural- and glial markers. Differentiation protocols are shown in bracket. (A) NESTIN (protocol 5), (D) TUJI (protocol 5). (G) TH (protocol 2). (J) GFAP (protocol 3). (M) O4 (protocol 4). (B, E, H, K, and N) Hoechst. (C, F, I, L and O) Merge of primary antibody staining and Hoechst. Scale bars represent 0.05 mm.

immunocytochemistry. The prevalence of these markers in most of the cells corroborates their NPC identity and points to a nearly homogeneous population. Furthermore, pluripotent cells did not seem to be present among the NPCs as staining for the pluripotency marker OCT4 was negative. To test the reproducibility of the method, two additional NPC lines were established and analyzed by immunocytochemistry, which showed a similar expression profile. Puy and colleagues found that porcine ICM-derived NPCs were positive for *SOX2*, *NESTIN* and *VIMENTIN* (Puy et al., 2010), which match our present findings very well. Nevertheless, the cellular phenotype of the NPCs did seem to change over a prolonged period of culture, as TUJI was observed in a higher number of cells at passage 15, whereas, PAX6 was not observed anymore. This could be attributed to in vitro maturation of the NPCs, which corresponds to what is observed in vivo, since embryonic and adult brain-derived NPCs show different expression profiles.

Analysis of Day 42 porcine fetal brain using immunohistochemistry showed expression of KI67, SOX2, NESTIN, VIMENTIN, and PAX6 in the VZ of the lateral ventricle, whereas, TUJI and NCAM were predominantly located in the MZ. Hence, the expression profile of the NPCs derived in this

study corresponds well with fetal NPCs located in the VZ. When Schwartz and colleagues analyzed porcine fetal-derived NPCs they also found expression of SOX2, VIMENTIN and NCAM, whereas NESTIN was not detected due to a lack of antibody specificity (Schwartz et al., 2005).

GFAP is a marker found in several different cell types. It is expressed in adult, but not in fetal-derived NPCs (Imura et al., 2003) and in concert with SSEA1, it is used to characterize radial glia in the brain (Mo et al., 2007; Howard et al., 2008). However, GFAP is also considered a marker of type 2 astrocytes (Talbot et al., 2002). Immunocytochemical analyses showed that the porcine NPCs were negative for both GFAP and SSEA1, indicating that they share more characteristics with fetal-derived NPCs from the VZ. In contrast, Puy and colleagues found GFAP staining in 13% of the porcine ICM-derived NPCs (Puy et al., 2010) and it is possible that these cells had already differentiated into the astrocyte lineage.

For cells to be characterized as multipotent NPCs, they must possess the ability to differentiate into both neural- and glial cells. To determine the differentiation potential of the NPCs, various combinations of growth factors known to promote differentiation of human NPCs into mature neurons and glia were tested. Generation of neurons from NPCs was most efficient in protocol 2, containing RA, SHH, BDNF and AA. This was not surprising since RA and SHH are known to play key roles in neural patterning in the early embryo (Patten and Placzek, 2000; Maden, 2007). Interestingly, TH, a marker of dopaminergic neurons, was also detected in protocol 2, whereas in protocol 3 (containing FGF8 and SHH for generation of dopaminergic neurons (Perrier et al., 2004)) TH positive cells were not observed. This could be due to species-specific differences in response to growth factors, however, it is more likely due to timing, as sequential application of FGF8 and SHH has been shown to promote formation of doperminergic midbrain neurons from human NPCs (Yan et al., 2005; Hong et al., 2008).

Oligodendrocyte progenitor cells were most abundant in protocol 4, containing PDGF, as detected by immunocytochemistry with O4. In contrast, expression of the oligodendrocyte marker *MBP* was significantly up-regulated in protocol 3, as detected by comparative real-time PCR. It is possible that an extended differentiation period as well as other factors such as BDNF, GDNF and AA is required for the final maturation to mature *MBP*-expressing oligodendrocytes. In the human, several authors have previously reported low quantities of oligodendrocytes from human ESC-derived NPCs (Reubinoff et al., 2001; Dhara et al., 2008). However, a protocol for generation of high amounts of oligodendrocyte progenitor cells from human ESCs has recently been published, which includes 10 days supplementation with RA and SHH followed by 20 days supplementation with bFGF and 2 months maturation in PDGF, Insulin-like growth factor 1 and Neurotrophin 3. This protocol could be interesting to apply to the porcine NPCs (Hu et al., 2009).

Astrocytes were generated in protocols 1 to 4, which is in agreement with the general dogma of spontaneous astrocyte formation (Trounson, 2006). Surprisingly, the combination of RA and LIF in protocol 5, which has been shown to yield high numbers of astrocytes from mouse NPCs (Asano et al., 2009), had the opposite effect in this study. In human, LIF has been shown to stimulate long-term culture of undifferentiated human NPCs (Andersen et al., 2009). Hence, it is possible that LIF was responsible for the inhibitory effect on astrocyte formation as it was the only factor included exclusively in protocol 5. For a thorough examination of the long-term plasticity of the NPCs, differentiation experiments using late stage NPCs are required; however, this lies beyond the scope of this study.

Accumulating evidence suggests that NPCs derived from early-stage cells and embryos possess superior plasticity compared to those derived from older stages. This is illustrated in a study by Chung and colleagues, in which mouse ESC-derived NPCs were able to differentiate into dopaminergic neurons in culture, whereas, fetal-derived NPCs from the ventral mesencephalon lacked this ability (Chung et al., 2006). Furthermore, transplantation of porcine NPCs derived from Day 22 and Day 27 embryos into a rat model of Parkinson's disease showed that only the early-stage cells survived the transplantation (Armstrong et al., 2003). In another study by Harrower and co-workers, a significantly improved survival and integration of in-vitro cultured porcine NPCs compared to primary porcine grafts in a rat model of Parkinson's disease were observed (Harrower et al., 2006). Hence, in-vitro culture could play an important role in resetting the NPCs to an earlier state, perhaps through erasure of immunological identity. Since the NPCs in this study are derived directly from the epiblast and cultured under in-vitro conditions, differentiation, integration and survival in the porcine brain might be favored compared to their in-vivo derived counterparts.

Conclusion

The porcine blastocyst-derived NPCs share many characteristics with human ESC-derived NPCs, such as expression of NPC markers, their capacity for long-term proliferation and ability to differentiate into both neurons and glia. As a result, they may be used in porcine brain transplantation studies as a model of allogeneic cell replacement therapy. Pigs are currently considered the standard experimental model for human brain development, due to their similar anatomical and physiological characteristics (Lind et al., 2007) and with the increasing number of porcine disease models emerging through nuclear transfer (Kragh et al., 2009) the pig would constitute an outstanding large animal model to study NPC-based treatment of neurodegenerative diseases.

Materials and methods

Unless otherwise stated, materials were purchased from Invitrogen, Carlsbad, CA.

Isolation and culture of epiblast cells

Uteri from four Danish sows (Landrace x Yorkshire crosses) were artificially inseminated over 2 days with semen from Duroc boars and collected at a local abattoir 9 days post insemination (Day 9). Each uterine horn was flushed with 150 ml embryo transfer solution (LIFE Pharmacy, KU, Frederiksberg, Denmark) containing 0.1% FBS and collected

via a flushing catheter. Embryos were subsequently isolated in DMEM containing HEPES (Sigma-Aldrich, St. Louis, MO) and 10% FCS by stereo-microscopy. Epiblasts were mechanically isolated from the surrounding trophectoderm and hypoblast of Day 9 expanded hatched blastocysts using insulin needles. The isolated epiblasts were cultured as outgrowth colonies (OCs) in dishes containing $2\times10^4/cm^2$ irradiation inactivated mouse embryonic fibroblast (MEF) feeder cells (DSMZ, Braunschweig, Germany) in ESC medium consisting of knockout DMEM (Sigma-Aldrich), 10% knockout serum replacement (KSR), 5% FCS, 1% penicillin/streptomycin (Sigma-Aldrich), 1% non-essential amino acids (Sigma-Aldrich), 0.2% beta-mercaptoethanol (Sigma-Aldrich), 20 ng/ml human bFGF and 20 ng/ml human Activin A (R&D systems, Minneapolis, MN) and cultured at 38 °C in 20% O_2, 5% CO_2 in N_2.

Derivation of porcine NPCs

MS5 stromal cells (MS5; DSMZ) were cultured for one day in gelatin-coated dishes in a medium consisting of alpha-MEM medium (Sigma-Aldrich) containing 10% FBS. On Day 5, following epiblast isolation, ESC-like areas of OCs were cut into 4–12 small pieces by use of insulin needles and co-cultured with $2\times10^4/cm^2$ MS5 cells in serum replacement medium containing DMEM, 15% KSR and 2 mM L-glutamine (Perrier et al., 2004). The cells were cultured at 38 °C in 20% O_2, 5% CO_2 in N_2 and medium was replaced every 2–3 days without passage. Rosettes, which typically appeared after 12–17 days co-culture, were isolated by insulin needles, cut into small pieces and transferred to Matrigel-coated dishes (BD Biosciences, Franklin Lakes, NJ) in medium containing DMEM/F12, 1xB-27 supplement, 1xN2 supplement, 20 ng/ml EGF (Prospec, Rehovot, Israel) and 20 ng/ml bFGF and cultured at 38 °C in 20% O_2, 5% CO_2 in N_2 with medium change every 2–3 days. After 8 days, the cells were disaggregated in 1% Trypsin/EDTA and split into new Matrigel-coated dishes (BD Biosciences) at a ratio of 1:5 (termed passage 1), with subsequent passage every 3–4 days. Cells from passage 5, 21 and 30 were sampled for comparative real-time PCR analysis and from passage 4 and 16 for immunocytochemical analysis.

Proliferation and karyotyping of NPCs

For analysis of cell doublings, trypsin treated cells were counted at each passage using a haemocytometer and total cell doublings were calculated (starting from passage 1). To check for cytogenetic abnormalities, karyotyping of NPCs at passage 7 was performed according to standard cytogenetic techniques. Briefly, a 100 mm culture dish of 65% confluent and dividing cells was treated with 0.1 μg/mL of colcemid (Sigma-Aldrich) for 25 min, trypsinized, resuspended in a pre-warmed hypotonic solution of 0.075 M KCl (Sigma-Aldrich) and incubated at 37 °C for 18 min. Cells were then fixed at room temperature by resuspending in freshly made 3:1 methanol:glacial acetic acid fixative (Sigma-Aldrich) and incubated for 1 h. Dry, clean slides were wetted with a drop of fixative and 15 μL of cellular suspension was dropped onto the surface and allowed to dry in a humid environment. Slides were aged in a dry oven at 90 °C for 1 h, cooled to room temperature, stained in 8% (v/v) Giemsa (Sigma-Aldrich) in Gurr buffer (pH 6.8) for 2–4 min, rinsed 3 times in H_2O and dried. Fourteen images of metaphases were captured using standard bright field microscopy and checked for cytogenetic abnormalities.

Differentiation of NPCs into neurons and glia

To evaluate the differentiation potential of the NPCs, five alternate differentiation protocols were performed. NPCs at passage 4 were disaggregated into single cells and seeded at a density of $1\times10^5/cm^2$ in Matrigel-coated dishes (BD Biosciences) and dishes containing Matrigel-coated glass coverslips (ThermoFisher Scientific, Waltham, MA). The cells were cultured for a total of three weeks in N2 medium consisting of DMEM/F12 and 1xN2 supplement in the following conditions: Protocol 1 (*mixed neurons and glia*); N2 medium without growth factors (Joannides et al., 2007). Protocol 2 (*motoneurons*); two weeks culture in N2 medium containing 1 μM all-*trans*-retinoic acid (RA; Sigma-Aldrich), 200 ng/ml recombinant murine sonic hedgehog (SHH), 20 ng/ml human recombinant brain-derived neurotrophic factor (BDNF, Prospec, Rehovot, Israel), 0.2 mM ascorbic acid (AA; Sigma-Aldrich) followed by one week maturation in 20 ng/ml human recombinant glial cell line-derived neurotrophic factor (GDNF, Prospec, Rehovot, Israel), 20 ng/ml BDNF (Prospec) and 0.2 mM AA (Sigma-Aldrich) (Lee et al., 2007). Protocol 3 (*Dopaminergic midbrain neurons*); two weeks culture in 200 ng/ml SHH, 100 ng/ml human recombinant fibroblast growth factor 8 (FGF8), 20 ng/ml BDNF (Prospec) and 0.2 mM AA (Sigma-Aldrich) followed by one week maturation in 20 ng/ml GDNF (Prospec) and 20 ng/ml BDNF (Prospec) and 0.2 mM AA (Sigma-Aldrich) (Perrier et al., 2004). Protocol 4 (*Oligodendrocytes*); 20 ng/ml human recombinant platelet-derived growth factor-AB (PDGF; Sigma-Aldrich) (Hu et al., 2008) and Protocol 5 (*Astrocytes*); 1 μM RA and 20 ng/ml recombinant murine leukemia inhibitory factor (LIF; Chemicon, Hessen, Germany) (Asano et al., 2009). Differentiation was performed at 38 °C in 5% O_2, 5% CO_2 in N_2, with half of the media changed every third day. Only cells in protocols 3 and 4 were passaged 1:2 on Day 9 due to continued proliferation. At the conclusion of the experiment, three samples were obtained from each protocol for comparative real-time PCR and two samples were obtained for immunocytochemistry.

RNA purification and reverse transcription

Neural progenitor cells and differentiated cells were trypsinized into single cells, placed in lysis buffer (Qiagen, Chatsworth, CA), snap-frozen in liquid nitrogen and stored at −80 °C. As positive control tissue, porcine brains from three fetuses, isolated from the uterus of a Danish sow (Landrace x Yorkshire crosses) 42 days post insemination (Day 42) (Vejlsted et al., 2006), were isolated from the skull and minced using a razorblade. As negative control tissue, MS5 cells were cultured as described above. Both were placed into lysis buffer, frozen in liquid nitrogen and stored at −80 °C. Total RNA was purified using the RNeasy mini or micro kit (Qiagen) and the RNA content and purity were measured on a Nanodrop 1000 spectrophotometer (ThermoFisher Scientific). Reverse transcription was performed using the RevertAid First strand cDNA synthesis kit (Fermentas, Burlington, ON) according to the manufacturer's instructions.

For each sample, a negative reaction was included, whereby the M-MuLV Reverse Transcriptase enzyme was omitted.

Comparative real-time PCR

Comparative real-time PCR using the ΔΔCT method was performed with a Lightcycler SW480 and SYBR Green I Master mix (Roche, Basal, Switzerland). PCR conditions were: 45 cycles of denaturation at 95 °C for 10 s, annealing at 58 °C for 10 s and elongation at 72 °C for 20 s. Porcine specific primers designed using alignment of porcine sequences with human genes or previously published primers was used (Suppl. Table 1). Three independent biological samples were analyzed which were each run in triplicate. H_2O and mouse MS5 cDNA served as negative controls and pooled brain cDNA from Day 42 porcine fetuses served as endogenous control tissue. Three different reference genes were tested on all the samples; glyceraldehyde 3-phosphate dehydrogenase (*GAPDH*) (Kuijk et al., 2007), Tata box binding protein 1 (*TBP1*) (Nygard et al., 2007) and phosphoglycerate kinase 1 (*PGK1*) (Boda et al., 2009). GeNorm (Vandesompele et al., 2002) and NormFinder (Andersen et al., 2004) were subsequently used to determine the most optimal reference gene.

Statistical analysis

Comparative real-time PCR samples were normalized using the ΔΔCt method. The ΔCT value was calculated by normalizing the CT value of the target gene with the CT value of the housekeeping gene. The ΔΔCT value was calculated by normalizing the ΔCT value to the reference tissue. Finally, the fold change in gene expression was determined by the equation $2^{-\Delta\Delta CT}$. In the differentiation experiment, calculation of standard deviations as well as statistical analysis was performed on the $2^{-\Delta\Delta CT}$ value using one way ANOVA to analyze the difference between treated and non-treated samples. Significance was determined as $p \leq 0.05$.

Fixation of cells and tissues

Neural progenitor cells and differentiated cells were cultured on Matrigel-coated (BD Biosciences) glass coverslips (ThermoFisher Scientific), fixed for 20 min in 4% PFA and stored in 1% PFA at 4 °C. As a positive control, a head from a Day 42 fetus was dissected and fixed overnight in 4% paraformaldehyde (PFA), frozen in Tissue-tek (Sakura Finetek, Torrance, CA), cut into 5 μm sections using a cryostat and stored at −80 °C. As a negative control tissue, MS5 cells were cultured as described above on Matrigel coated (BD Biosciences) glass coverslips (ThermoFisher Scientific), fixed for 20 min in 4% PFA and stored in 1% PFA at 4 °C.

Immunocytochemistry

Immunocytochemistry was performed as follows: 30 min permeabilization in 0.1% Triton X-100 (Sigma-Aldrich), 1 h blocking in PBS containing 5% Donkey serum (Sigma-Aldrich) and incubation over night at 4 °C with primary antibodies (Suppl. Table 2) in 0.25% BSA (Sigma-Aldrich), 0.1% Triton X-100 in PBS. The following day, cells were washed 3 times in PBS, incubated for 1 h with fluorescent-conjugated secondary antibodies (Alexa Fluor; 1:400) diluted in 0.25% BSA, 0.1% Triton X-100 in PBS, washed 3 times in PBS, incubated in 0.1 μl/ml Bisbenzimide Hoechst (Sigma-Aldrich) and mounted in fluorescence mounting medium (Dako, Glostrup, Denmark). The OCs were used to verify specificity of pluripotency markers and the brain of a Day 42 porcine fetus was prepared as described above and used to verify specificity of neuronal antibodies. Mouse MS5 cells were included as a negative control. All specimens were examined using a Leica DMRB fluorescent microscope and Leica Application Suite 2.81 (Leica Microsystems). For quantification of positive antibody labeling of undifferentiated and differentiated cells, a minimum of 500 Hoechst-stained cells per treatment per antibody staining were counted from eight different, equally distributed locations on a glass coverslip and compared to the number of cells with positive staining using ImageJ (Collins, 2007). In total, 15.500 cells were counted.

Supplementary materials related to this article can be found online at doi:10.1016/j.scr.2011.04.004.

Acknowledgments

The authors would like to thank Postdoc Stoyan Petkov for assisting in cell culture and Assistant Professors Kirsten Schauser and Morten Meyer for guidance in antibody staining procedures. Finally we acknowledge the financial support of EU projects, from the 7th Framework, PluriSyS (223485) and PartnErS (218205) as well as from the Danish National Advanced Technology Foundation, Pigs and Health project, in Denmark.

References

Amariglio, N., Hirshberg, A., Scheithauer, B.W., Cohen, Y., Loewenthal, R., Trakhtenbrot, L., Paz, N., Koren-Michowitz, M., Waldman, D., Leider-Trejo, L., Toren, A., Constantini, S., Rechavi, G., 2009. Donor-derived brain tumor following neural stem cell transplantation in an ataxia telangiectasia patient. PLoS Med. 6, e1000029.

Andersen, C.L., Jensen, J.L., Orntoft, T.F., 2004. Normalization of real-time quantitative reverse transcription-PCR data: a model-based variance estimation approach to identify genes suited for normalization, applied to bladder and colon cancer data sets. Cancer Res. 64, 5245–5250.

Andersen, R.K., Widmer, H.R., Zimmer, J., Wahlberg, L.U., Meyer, M., 2009. Leukemia inhibitory factor favours neurogenic differentiation of long-term propagated human midbrain precursor cells. Neurosci. Lett. 464, 203–208.

Armstrong, R.J., Tyers, P., Jain, M., Richards, A., Dunnett, S.B., Rosser, A.E., Barker, R.A., 2003. Transplantation of expanded neural precursor cells from the developing pig ventral mesencephalon in a rat model of Parkinson's disease. Exp. Brain Res. 151, 204–217.

Asano, H., Aonuma, M., Sanosaka, T., Kohyama, J., Namihira, M., Nakashima, K., 2009. Astrocyte differentiation of neural precursor cells is enhanced by retinoic acid through a change in epigenetic modification. Stem Cells 27, 2744–2752.

Barberi, T., Klivenyi, P., Calingasan, N.Y., Lee, H., Kawamata, H., Loonam, K., Perrier, A.L., Bruses, J., Rubio, M.E., Topf, N., Tabar, V., Harrison, N.L., Beal, M.F., Moore, M.A., Studer, L., 2003. Neural subtype specification of fertilization and nuclear

transfer embryonic stem cells and application in parkinsonian mice. Nat. Biotechnol. 21, 1200–1207.
Bjarkam, C.R., Nielsen, M.S., Glud, A.N., Rosendal, F., Mogensen, P., Bender, D., Doudet, D., Moller, A., Sorensen, J.C., 2008. Neuromodulation in a minipig MPTP model of Parkinson disease. Br. J. Neurosurg. 22 (Suppl. 1), 9–12.
Blurton-Jones, M., Kitazawa, M., Martinez-Coria, H., Castello, N.A., Muller, F.J., Loring, J.F., Yamasaki, T.R., Poon, W.W., Green, K.N., LaFerla, F.M., 2009. Neural stem cells improve cognition via BDNF in a transgenic model of Alzheimer disease. Proc. Natl. Acad. Sci. U. S. A. 106, 13594–13599.
Boda, E., Pini, A., Hoxha, E., Parolisi, R., Tempia, F., 2009. Selection of reference genes for quantitative real-time RT-PCR studies in mouse brain. J. Mol. Neurosci. 37, 238–253.
Chung, S., Shin, B.S., Hwang, M., Lardaro, T., Kang, U.J., Isacson, O., Kim, K.S., 2006. Neural precursors derived from embryonic stem cells, but not those from fetal ventral mesencephalon, maintain the potential to differentiate into dopaminergic neurons after expansion in vitro. Stem Cells 24, 1583–1593.
Collins, T.J., 2007. ImageJ for microscopy. Biotechniques 43, 25–30.
Dhara, S.K., Hasneen, K., Machacek, D.W., Boyd, N.L., Rao, R.R., Stice, S.L., 2008. Human neural progenitor cells derived from embryonic stem cells in feeder-free cultures. Differentiation 76, 454–464.
Esteban, M.A., Xu, J., Yang, J., Peng, M., Qin, D., Li, W., Jiang, Z., Chen, J., Deng, K., Zhong, M., Cai, J., Lai, L., Pei, D., 2009. Generation of induced pluripotent stem cell lines from Tibetan miniature pig. J. Biol. Chem. 284, 17634–17640.
Ezashi, T., Telugu, B.P., Alexenko, A.P., Sachdev, S., Sinha, S., Roberts, R.M., 2009. Derivation of induced pluripotent stem cells from pig somatic cells. Proc. Natl. Acad. Sci. U.S.A. 106, 10993–10998.
Geeta, R., Ramnath, R.L., Rao, H.S., Chandra, V., 2008. One year survival and significant reversal of motor deficits in parkinsonian rats transplanted with hESC derived dopaminergic neurons. Biochem. Biophys. Res. Commun. 373, 258–264.
Harrower, T.P., Tyers, P., Hooks, Y., Barker, R.A., 2006. Long-term survival and integration of porcine expanded neural precursor cell grafts in a rat model of Parkinson's disease. Exp. Neurol. 197, 56–69.
Hong, S., Kang, U.J., Isacson, O., Kim, K.S., 2008. Neural precursors derived from human embryonic stem cells maintain long-term proliferation without losing the potential to differentiate into all three neural lineages, including dopaminergic neurons. J. Neurochem. 104, 316–324.
Howard, B.M., Zhicheng, M., Filipovic, R., Moore, A.R., Antic, S.D., Zecevic, N., 2008. Radial glia cells in the developing human brain. Neuroscientist 14, 459–473.
Hu, J.G., Fu, S.L., Wang, Y.X., Li, Y., Jiang, X.Y., Wang, X.F., Qiu, M.S., Lu, P.H., Xu, X.M., 2008. Platelet-derived growth factor-AA mediates oligodendrocyte lineage differentiation through activation of extracellular signal-regulated kinase signaling pathway. Neuroscience 151, 138–147.
Hu, B.Y., Du, Z.W., Zhang, S.C., 2009. Differentiation of human oligodendrocytes from pluripotent stem cells. Nat. Protoc. 4, 1614–1622.
Imura, T., Kornblum, H.I., Sofroniew, M.V., 2003. The predominant neural stem cell isolated from postnatal and adult forebrain but not early embryonic forebrain expresses GFAP. J. Neurosci. 23, 2824–2832.
Joannides, A.J., Fiore-Heriche, C., Battersby, A.A., thauda-Arachchi, P., Bouhon, I.A., Williams, L., Westmore, K., Kemp, P.J., Compston, A., Allen, N.D., Chandran, S., 2007. A scaleable and defined system for generating neural stem cells from human embryonic stem cells. Stem Cells 25, 731–737.
Kragh, P.M., Nielsen, A.L., Li, J., Du, Y., Lin, L., Schmidt, M., Bogh, I.B., Holm, I.E., Jakobsen, J.E., Johansen, M.G., Purup, S., Bolund, L., Vajta, G., Jorgensen, A.L., 2009. Hemizygous minipigs produced by random gene insertion and handmade cloning express the Alzheimer's disease-causing dominant mutation APPsw. Transgenic Res. 18, 545–558.
Kuijk, E.W., Du, P.L., van Tol, H.T., Haagsman, H.P., Colenbrander, B., Roelen, B.A., 2007. Validation of reference genes for quantitative RT-PCR studies in porcine oocytes and preimplantation embryos. BMC Dev. Biol. 7, 58.
Lazzari, G., Colleoni, S., Giannelli, S.G., Brunetti, D., Colombo, E., Lagutina, I., Galli, C., Broccoli, V., 2006. Direct derivation of neural rosettes from cloned bovine blastocysts: a model of early neurulation events and neural crest specification in vitro. Stem Cells 24, 2514–2521.
Lee, G., Kim, H., Elkabetz, Y., Al, S.G., Panagiotakos, G., Barberi, T., Tabar, V., Studer, L., 2007. Isolation and directed differentiation of neural crest stem cells derived from human embryonic stem cells. Nat. Biotechnol. 25, 1468–1475.
Lepore, A.C., Rauck, B., Dejea, C., Pardo, A.C., Rao, M.S., Rothstein, J.D., Maragakis, N.J., 2008. Focal transplantation-based astrocyte replacement is neuroprotective in a model of motor neuron disease. Nat. Neurosci. 11, 1294–1301.
Lind, N.M., Moustgaard, A., Jelsing, J., Vajta, G., Cumming, P., Hansen, A.K., 2007. The use of pigs in neuroscience: modeling brain disorders. Neurosci. Biobehav. Rev. 31, 728–751.
Ma, D.K., Bonaguidi, M.A., Ming, G.L., Song, H., 2009. Adult neural stem cells in the mammalian central nervous system. Cell Res. 19, 672–682.
Maden, M., 2007. Retinoic acid in the development, regeneration and maintenance of the nervous system. Nat. Rev. Neurosci. 8, 755–765.
Maisel, M., Herr, A., Milosevic, J., Hermann, A., Habisch, H.J., Schwarz, S., Kirsch, M., Antoniadis, G., Brenner, R., Hallmeyer-Elgner, S., Lerche, H., Schwarz, J., Storch, A., 2007. Transcription profiling of adult and fetal human neuroprogenitors identifies divergent paths to maintain the neuroprogenitor cell state. Stem Cells 25, 1231–1240.
Mehler, M.F., Kessler, J.A., 1999. Progenitor cell biology: implications for neural regeneration. Arch. Neurol. 56, 780–784.
Mo, Z., Moore, A.R., Filipovic, R., Ogawa, Y., Kazuhiro, I., Antic, S.D., Zecevic, N., 2007. Human cortical neurons originate from radial glia and neuron-restricted progenitors. J. Neurosci. 27, 4132–4145.
Nielsen, M.S., Sorensen, J.C., Bjarkam, C.R., 2009. The substantia nigra pars compacta of the Gottingen minipig: an anatomical and stereological study. Brain Struct. Funct. 213, 481–488.
Nygard, A.B., Jorgensen, C.B., Cirera, S., Fredholm, M., 2007. Selection of reference genes for gene expression studies in pig tissues using SYBR green qPCR. BMC Mol. Biol. 8, 67.
Oberheim, N.A., Takano, T., Han, X., He, W., Lin, J.H., Wang, F., Xu, Q., Wyatt, J.D., Pilcher, W., Ojemann, J.G., Ransom, B.R., Goldman, S.A., Nedergaard, M., 2009. Uniquely hominid features of adult human astrocytes. J. Neurosci. 29, 3276–3287.
Oh, S., Tseng, G.C., Sibille, E., 2009. Reciprocal phylogenetic conservation of molecular aging in mouse and human brain. Neurobiol. Aging (Electronic publication ahead of print) doi:10.1016/j.neurobiolaging.2009.08.004.
O'Keeffe, G.C., Tyers, P., Aarsland, D., Dalley, J.W., Barker, R.A., Caldwell, M.A., 2009. Dopamine-induced proliferation of adult neural precursor cells in the mammalian subventricular zone is mediated through EGF. Proc. Natl. Acad. Sci. U. S. A. 106, 8754–8759.
Patten, I., Placzek, M., 2000. The role of Sonic hedgehog in neural tube patterning. Cell. Mol. Life Sci. 57, 1695–1708.
Perrier, A.L., Tabar, V., Barberi, T., Rubio, M.E., Bruses, J., Topf, N., Harrison, N.L., Studer, L., 2004. Derivation of midbrain dopamine neurons from human embryonic stem cells. Proc. Natl. Acad. Sci. U. S. A. 101, 12543–12548.
Pluchino, S., Quattrini, A., Brambilla, E., Gritti, A., Salani, G., Dina, G., Galli, R., Del, C.U., Amadio, S., Bergami, A., Furlan, R., Comi, G., Vescovi, A.L., Martino, G., 2003. Injection of adult neurospheres

induces recovery in a chronic model of multiple sclerosis. Nature 422, 688–694.

Puy, L., Chuva de Sousa Lopes, S.M., Haagsman, H.P., Roelen, B.A., 2010. Differentiation of porcine inner cell mass cells into proliferating neural cells. Stem Cells Dev. 19, 61–70.

Reubinoff, B.E., Itsykson, P., Turetsky, T., Pera, M.F., Reinhartz, E., Itzik, A., Ben-Hur, T., 2001. Neural progenitors from human embryonic stem cells. Nat. Biotechnol. 19, 1134–1140.

Roy, N.S., Cleren, C., Singh, S.K., Yang, L., Beal, M.F., Goldman, S.A., 2006. Functional engraftment of human ES cell-derived dopaminergic neurons enriched by coculture with telomerase-immortalized midbrain astrocytes. Nat. Med. 12, 1259–1268.

Schwartz, P.H., Nethercott, H., Kirov, I.I., Ziaeian, B., Young, M.J., Klassen, H., 2005. Expression of neurodevelopmental markers by cultured porcine neural precursor cells. Stem Cells 23, 1286–1294.

Shin, S., Sun, Y., Liu, Y., Khaner, H., Svant, S., Cai, J., Xu, Q.X., Davidson, B.P., Stice, S.L., Smith, A.K., Goldman, S.A., Reubinoff, B.E., Zhan, M., Rao, M.S., Chesnut, J.D., 2007. Whole genome analysis of human neural stem cells derived from embryonic stem cells and stem and progenitor cells isolated from fetal tissue. Stem Cells 25, 1298–1306.

Sun, Y., Kong, W., Falk, A., Hu, J., Zhou, L., Pollard, S., Smith, A., 2009. CD133 (Prominin) negative human neural stem cells are clonogenic and tripotent. PLoS One 4, e5498.

Talbot, N.C., Powell, A.M., Garrett, W.M., 2002. Spontaneous differentiation of porcine and bovine embryonic stem cells (epiblast) into astrocytes or neurons. In Vitro Cell. Dev. Biol. Anim. 38, 191–197.

Trounson, A., 2006. The production and directed differentiation of human embryonic stem cells. Endocr. Rev. 27, 208–219.

Vackova, I., Ungrova, A., Lopes, F., 2007. Putative embryonic stem cell lines from pig embryos. J. Reprod. Dev. 53, 1137–1149.

Vandesompele, J., De, P.K., Pattyn, F., Poppe, B., Van, R.N., De, P.A., Speleman, F., 2002. Accurate normalization of real-time quantitative RT-PCR data by geometric averaging of multiple internal control genes. Genome Biol. 3 RESEARCH0034.

Vejlsted, M., Du, Y., Vajta, G., Maddox-Hyttel, P., 2006. Post-hatching development of the porcine and bovine embryo–defining criteria for expected development in vivo and in vitro. Theriogenology 65, 153–165.

Wu, Z., Chen, J., Ren, J., Bao, L., Liao, J., Cui, C., Rao, L., Li, H., Gu, Y., Dai, H., Zhu, H., Teng, X., Cheng, L., Xiao, L., 2009. Generation of pig induced pluripotent stem cells with a drug-inducible system. J. Mol. Cell Biol. 1, 46–54.

Yan, Y., Yang, D., Zarnowska, E.D., Du, Z., Werbel, B., Valliere, C., Pearce, R.A., Thomson, J.A., Zhang, S.C., 2005. Directed differentiation of dopaminergic neuronal subtypes from human embryonic stem cells. Stem Cells 23, 781–790.

Yang, D., Zhang, Z.J., Oldenburg, M., Ayala, M., Zhang, S.C., 2008. Human embryonic stem cell-derived dopaminergic neurons reverse functional deficit in parkinsonian rats. Stem Cells 26, 55–63.